THE JOURNAL OF BIOLOGICAL CHEMISTRY VOL. 289, NO. 52, pp. 35939–35952, December 26, 2014

A Role for *Saccharomyces cerevisiae* Tpa1 Protein in Direct Alkylation Repair*

Received for publication, June 18, 2014, and in revised form, November 6, 2014 Published, JBC Papers in Press, November 7, 2014, DOI 10.1074/jbc.M114.590216

Gururaj Shivange[1], **Naveena Kodipelli**[1], **Mohan Monisha, and Roy Anindya**[2]

From the Department of Biotechnology, Indian Institute of Technology Hyderabad, Ordnance Factory Estate, Yeddumailaram 502205, Hyderabad, India

Background: Fe(II)/2-oxoglutarate (2OG)-dependent dioxygenases repair alkyl-base lesions of DNA.
Results: Tpa1 is a Fe(II)/2OG-dependent dioxygenase and mediates alkyl-base repair in *Saccharomyces cerevisiae*, and deleting *TPA1* with DNA glycosylase *MAG1* had a synergistic effect on the susceptibility to methylation-induced toxicity.
Conclusion: Tpa1 protein plays a crucial role in DNA alkylation repair.
Significance: Our results provide the first evidence of direct alkylation repair by any Fe(II)/2OG-dependent dioxygenases in *Saccharomyces cerevisiae.*

Alkylating agents induce cytotoxic DNA base adducts. In this work, we provide evidence to suggest, for the first time, that *Saccharomyces cerevisiae* Tpa1 protein is involved in DNA alkylation repair. Little is known about Tpa1 as a repair protein beyond the initial observation from a high-throughput analysis indicating that deletion of *TPA1* causes methyl methane sulfonate sensitivity in *S. cerevisiae*. Using purified Tpa1, we demonstrate that Tpa1 repairs both single- and double-stranded methylated DNA. Tpa1 is a member of the Fe(II) and 2-oxoglutarate-dependent dioxygenase family, and we show that mutation of the amino acid residues involved in cofactor binding abolishes the Tpa1 DNA repair activity. Deletion of *TPA1* along with the base excision repair pathway DNA glycosylase *MAG1* renders the *tpa1Δmag1Δ* double mutant highly susceptible to methylation-induced toxicity. We further demonstrate that the trans-lesion synthesis DNA polymerase Polζ (*REV3*) plays a key role in tolerating DNA methyl-base lesions and that *tpa1Δmag1revΔ3* triple mutant is extremely susceptible to methylation-induced toxicity. Our results indicate a synergism between the base excision repair pathway and direct alkylation repair by Tpa1 in *S. cerevisiae.* We conclude that Tpa1 is a hitherto unidentified DNA repair protein in yeast and that it plays a crucial role in reverting alkylated DNA base lesions and cytotoxicity.

The genomes of every cell are always exposed to DNA-damaging alkylating agents that occur in the environment and are also generated endogenously as a byproduct of cellular oxidative metabolism. Some alkylating agents are also used in cancer chemotherapy (1). Simple methylating agents, such as MMS,[3] methylate double-stranded DNA and generate 7-methylguanine and 3-methyladenine (3meA) (2). DNA synthesis is blocked by 3meA, and it is considered a lethal lesion. Methylation of single-stranded DNA by MMS generates 1-methyladenine and 3-methylcytosine (3). In double-stranded DNA, these sites are protected by base pairing, but they can be transiently exposed during replication, transcription, or recombination. Therefore, the major genotoxicity of MMS is caused by three main lesions: 3meA, 1-methyladenine, and 3-methylcytosine (3, 4). Because replicative polymerases are stalled at these lesions, specialized damage-tolerant DNA polymerases are able to execute trans-lesion synthesis (TLS) (5). In *Saccharomyces cerevisiae*, TLS is carried out by the Polη (Rad30), Polζ (Rev3, Rev7), and Rev1 polymerases, all of which have human homologs (6). Yeast Polη is dedicated to the repair of UV light-induced cyclobutane-pyrimidine dimers in an error-free manner (7). In contrast, Pol ζ, in cooperation with Rev1, participates in error-prone TLS across lesions produced by variety of DNA-damaging agents, including MMS (8). In yeast, the DNA glycosylase Mag1 specifically removes 3meA. Following the Mag1-mediated removal of the damaged base, Apn1 apurinic/apyrimidinic endonuclease cleaves the DNA strand at the abasic site for subsequent repair of the single strand break by the base excision repair (BER) pathway. The enzyme that directly repairs 1-methyladenine and 3-methylcytosine is known as alkylation repair protein B (AlkB) in *Escherichia coli* (9, 10). AlkB deficient *E. coli* cells accumulate alkylated lesions and are hypersensitive to alkylating agents (11). The AlkB-catalyzed demethylation reaction is coupled to the oxidative decarboxylation of 2OG to succinate and CO_2, resulting in the removal of the methyl group from 1-methyladenine and 3-methylcytosine. The methyl group is hydroxylated and spontaneously released as formaldehyde (12, 13). AlkB is a member of the large Fe(II) and 2OG-dependent dioxygenase family and shows similar conserved features, like a conserved $HXDX_nH$ motif, that coordinate 2OG and iron and a catalytic core consisting of a double strand β-helix fold (14, 15).

* This work was supported by Innovative Young Biotechnologist Award Fellowship (2008) from the Department of Biotechnology, Government of India (to A. R.).
[1] Both authors contributed equally to this work.
[2] To whom correspondence should be addressed: Dept. of Biotechnology, Indian Institute of Technology Hyderabad, Ordnance Factory Estate, Yeddumailaram 502205, Hyderabad, India. Tel.: 91-40-23016083; Fax: 91-40-23016032; E-mail: anindya@iith.ac.in.
[3] The abbreviations used are: MMS, methyl methane sulfonate; 3meA, 3-methyladenine; TLS, trans-lesion synthesis; BER, base excision repair; 2OG, 2-oxoglutarate; NTD, N-terminal domain; CTD, C-terminal domain; FDH, formaldehyde dehydrogenase; YPD, yeast extract peptone dextrose; HIF, hypoxia-inducible factor.

Homologs of AlkB were identified across species ranging from bacteria to human (16, 17), except for *S. cerevisiae* (18). It has been reported earlier that two genes of *S. cerevisiae*, *YFW1* and *YFW12*, could complement the deficiency of AlkB in *E. coli* (19). However, *YFW1* is an endoplasmic reticulum membrane protein, and *YFW12* is a secreted sterol binding protein, and they share no sequence homology with AlkB or any other Fe(II)- and 2OG-dependent dioxygenases (20, 21). Therefore, they could not be considered AlkB homologs. No genetic interactions were reported Although the functional homolog of AlkB remained unknown in *S. cerevisiae*, a search for the dioxygenase domain-containing proteins in budding yeast revealed that an uncharacterized ORF named *YER049W* had the characteristic dioxygenase domain (22). Later, the gene product of *YER049W* was renamed termination and polyadenylation protein (Tpa1) because it was found to be associated with eRF1, eRF3, and polyA binding protein within the mRNA ribonucleoprotein complex (23). TPA1 deletion in yeast resulted in a decrease of translation termination efficacy and an increase in mRNAs stability (24). Structural analysis of Tpa1 revealed the presence of two domains: the N-terminal domain (NTD) and the C-terminal domain (CTD) (24, 25). Although the conserved double strand β-helix fold was found in both domains, only NTD was found to have bound iron (23). A recent study demonstrated that Tpa1 probably functions as a prolylhydroxylase responsible for hydroxylation of the 40 S ribosomal subunit protein (26). However, none of these studies provided any direct evidence for prolylhydroxylase enzymatic activity using purified Tpa1 (24–26).

This study was initiated in response to the findings that Tpa1 is the only *S. cerevisiae* protein that belongs to Fe(II) and 2OG-dependent dioxygenase superfamily of proteins, which also includes AlkB (22). Furthermore, a genetic screen in yeast deletion mutants revealed that TPA1 deletion caused mild MMS sensitivity (27), making it even more pressing to know the importance, if any, of this protein in the repair of DNA alkylation damage. Here we provide evidence that purified recombinant Tpa1 catalyzes the oxidative demethylation of methylated DNA and promote survival of MMS-sensitive *E. coli alkB* mutant cells. Furthermore, we demonstrate a genetic interaction between Tpa1, the DNA glycosylase Mag1, and TLS polymerases Polζ (Rev3) in *S. cerevisiae*. We also show that Mag1 appears to have a synergistic relationship with Tpa1 because the *tpa1*Δ*mag1*Δ double mutant showed an exacerbated phenotype. Most notably, we uncovered a remarkable synergism among Mag1, Tpa1, and TLS polymerases Polζ (Rev3) in protecting against methylation damage, as indicated by the inability of the *tpa1*Δ*mag1*Δ*rev3*Δ triple mutant cells to recover from extremely low level of MMS-induced methylation damage.

EXPERIMENTAL PROCEDURES

Plasmid Constructs—For expression of recombinant proteins, all plasmids were constructed in the expression vector pGex6p1 (GE Healthcare) in-frame with an N-terminal GST. The *TPA1* gene was PCR-amplified from an *S. cerevisiae* genomic DNA using the appropriate primers. Similarly, the *E. coli* AlkB gene was PCR-amplified from *E. coli* genomic DNA. The Tpa1 NTD, which lacks amino acids 269–644, and the CTD, which lacks amino acids 1–276, were also PCR-amplified using specific primers. The PCR products of Tpa1, the NTD, the CTD, and AlkB were cloned into the BamHI and SalI sites of the pGex6p1 vector to yield pGex-Tpa1, pGex-Tpa1^{NTD}, pGex-Tpa1^{CTD}, and pGex-AlkB, respectively.

To generate mutant Tpa1, PyMOL was used to make the substitution mutations *in silico* using the PyMOL Mutagenesis Wizard. A molecular docking analysis was performed to confirm whether cofactor binding is indeed abolished using published structures of Tpa1 (24, 25). Initially, to assess the reliability of the docking method, 2OG was removed from the holoenzyme atomic structure (PDB code 3KT7), and then the coordinates of 2OG were docked back into the rigid binding site. On the basis of the Tpa1 structure and molecular docking analysis, we determined the amino acid residues involved in coordinating the iron in the active site. Accordingly, we introduced a site-specific mutations into the recombinant Tpa1 active site using the protein variation effect analyzer algorithm (28). H159C, D161N, H227C, H237C, and R238A were introduced to generate pGex-Tpa1^{mut}. The FoldX algorithm was used to make sure that the mutations did not affect the overall stability of the protein (29).

Functional Complementation of alkB Mutant E. coli—Functional complementation of *E. coli* HK82 (*alkB*) cells (30) was carried out as described before, with some modifications (31). HK82 competent cells were transformed with either pGex-Tpa1, pGex-Tpa1^{NTD}, pGex-Tpa1^{CTD}, or pGex-AlkB. Cells were grown in Luria Broth medium containing ampicillin at 37 °C. Protein expression was induced by adding 1 mM isopropyl 1-thio-β-D-galactopyranoside to the medium, followed by further incubation for 4 h. The expression was confirmed by SDS-PAGE analysis. For this, 1 ml of cultures from the induced cells was harvested by centrifugation, resuspended in protein gel loading buffer, and incubated at 95 °C for 5 min, and then chromosomal DNA was removed by centrifugation and the lysate was analyzed on a 12% polyacrylamide gel. For survival analysis, cells were treated with 0.1% (v/v) MMS for 3 h. Excess MMS was removed by washing the cells with water. Finally, cells were plated on LB agar and incubated at 37 °C for 20 h.

Cell Survival Assay—Alkylation-induced cell killing was estimated by colony-forming ability. *E. coli* HK82 (*alkB*) cells transformed with either pGex-Tpa1, pGex-Tpa1^{NTD}, pGex-Tpa1^{CTD}, or pGex-AlkB were grown in LB medium at 37 °C. Cultures were treated with 0.05%, 0.1%, and 0.15% (v/v) MMS for 2 h, diluted, and spread on LB agar plates. Colonies were counted 20 h later, and survival was expressed as a percentage of colonies where no MMS was present.

Purification of Recombinant Proteins—Plasmids were transformed into the *E. coli* strain BL21-CodonPlus(DE3)-RIL (Stratagene), and protein expression was induced by the addition of 1 mM isopropyl 1-thio-β-D-galactopyranoside. Cells were disrupted by sonication, and proteins were purified using affinity purification using glutathione-Sepharose 4B medium (GE Healthcare) (32). Proteins were analyzed by 12% SDS-PAGE and, subsequently, by Coomassie Brilliant Blue staining, and concentrations were determined by Bradford assays (Bio-Rad).

UV-visible Spectroscopy—UV-visible spectra of Tpa1, the Tpa1 mutant, the NTD, and the CTD were determined as described before (33). Briefly, recombinant proteins were purified as described before (32, 34) and concentrated to 0.04 μM. Spectra were recorded in the presence of buffer containing 25 mM Tris-HCl (pH 8.0), 50 mM KCl, 0.5 mM 2OG, 4.0 mM sodium ascorbate, and 880 μM $FeSO_4$ by using a Hitachi model UV-3900 spectrophotometer.

Preparation of Methylated DNA—Desalted oligonucleotides were purchased from Imperial Lifescience. Single-stranded DNA was purchased from Sigma (catalog no. D8899). Methylation adducts were generated by treating the oligonucleotide or single-stranded DNA with MMS (Sigma, catalog no. 129925), as described before (35). Briefly, 40 μg of single-stranded DNA oligonucleotides were incubated with 5% (v/v) (0.59 M) MMS and 200 mM K_2HPO_4 in 500 μl of the total reaction for 170 min at room temperature. Excess MMS was removed by dialysis against TE buffer (10 mM Tris-HCl (pH 8.0) and 1 mM EDTA) using a Spectra/Por dialysis membrane (molecular weight cut-off 3500 Da). Then the damaged substrate was precipitated by adding 0.3 M sodium acetate (pH 5.5) and 2 volumes of ice-cold ethanol. The precipitated single-stranded DNA was washed with 70% ethanol and finally dissolved in water.

Analysis of Tpa1 Demethylation Activity by Direct Detection of Formaldehyde—Formaldehyde reacts with ammonia and acetoacetanilide to form a fluorescent dihydropyridine product (36). The resulting fluorescent product could be analyzed using an excitation wavelength of 365 nm and an emission wavelength of 465 nm.

Direct detection of formaldehyde was carried out as follows. To a 50-μl sample containing formaldehyde, 40 μl of ammonium acetate (2 M) and 10 μl of acetoacetanilide (0.5 M) were added (0.05 M) to make the final volume 100 μl. The fluorescent compound was allowed to develop at 30 °C for 30 min, and fluorescence emission was measured at 465 nm using an excitation wavelength of 365 nm with a Spectramax multimode reader. For the quantification of formaldehyde release, a standard curve was generated using pure formaldehyde.

DNA demethylase assays (50 μl) were performed in 96-well dark plates (Corning) in the presence of demethylase buffer (20 mM HEPES (pH 8.0), 200 μM 2OG, 2 mM L-ascorbate, 20 μM $Fe(NH_4)_2(SO_4)_2$, and 100 μg/ml bovine serum albumin), MMS-treated methylated DNA (100 ng/μl), and purified proteins, *viz.* Tpa1, Tpa-mutant, or AlkB (2 μM), at 30 °C for 60 min.

Analysis of Tpa1 Demethylation Activity by FDH-coupled Assay—Formaldehyde production was continuously monitored by a formaldehyde dehydrogenase-coupled DNA repair assay. This assay was performed by incubating purified recombinant proteins, *viz.* Tpa1, mutant-TPA1, Tpa1-NTD, and Tpa1-CTD (2 μM), with the reaction buffer (20 mM HEPES (pH 8.0), 200 μM 2OG, 2 mM L-ascorbate, 20 μM $Fe(NH_4)_2(SO_4)_2$, and 100 μg/ml BSA) in the presence of damaged single-stranded DNA (10 ng/μl) in a total volume of 100 μl. The reaction mixture also contained 0.01 unit of FDH and 1 mM NAD^+ and was monitored continuously for the production of NADH (peak absorption at 340 nm) using a Spectramax multimode reader. Typically, three reactions were monitored concurrently for 30 min, each set containing one control (no DNA). The data were analyzed using GraphPad Prism software.

Analysis of Tpa1 Demethylation Activity by Methylation-sensitive Restriction Endonuclease-based Assay—For this assay, the sequence of the oligonucleotide selected for methylation was 5′-GGA TGC CTT CGA CAC CTA GCT TTG TTA GGT CTG GATC CTC GAA ATA CAA AGA TTG TAC TGA GAG TGC ACC-3′ (the MboI site is underlined). This 70-base oligonucleotide was designed so that, upon annealing with the complementary oligonucleotide, an MboI restriction site is formed in the middle. Restriction digestion of this 70-bp oligonucleotide with MboI would result in two 35-bp fragments. Because MboI digestion is inhibited by DNA methylation, including 1-methyladenine and 3-methylcytosine, restriction digestion of methylated oligonucleotide would not yield any 35-bp fragments. However, upon repair of this methylated substrate, it becomes susceptible to MboI digestion. In other words, MboI digestion of methylated substrate would indicate successful DNA repair. DNA repair was carried out by incubating recombinant Tpa1 (0.8 μM) or Tpa1 mutant (0.8 μM) with 3.7 μg of MMS-damaged, single-stranded oligonucleotide for 2 h at 30 °C in the presence of repair buffer (20 mM HEPES (pH 8.0), 200 μM 2-oxoglutarate, 2 mM L-ascorbic acid, 20 μM $Fe(NH_4)_2(SO_4)_2$, and 100 μg/ml BSA) in a total reaction volume of 25 μl. Following the repair reaction, the complementary strand was allowed to anneal with the repaired strand for 30 min at 30 °C. The resulting double-stranded DNA was cleaved with 2.5 units of the methylation-sensitive restriction enzyme MboI (New England Biolabs, catalog no. R0147) at 37 °C for 1 h. Tpa1-mediated removal of methyl adducts was determined by the appearance of a 35-bp band because of cleavage of the 70-bp oligonucleotide by MboI by agarose gel electrophoresis, as described before (35).

Yeast Strains and Procedures—All *S. cerevisiae* strains used were isogenic with strain W303 (*MATa; ura3–1 ade2–1 his3–11,5 trp1–1 leu2–3,112 can1–100*) (37). The cells were grown and manipulated using standard techniques (38). The *TPA1* gene was replaced with the *HIS3* gene by a one-step replacement. The *HIS3* gene was amplified from plasmid pRS303 (39) by using the specific primers so that the PCR product contained the entire *HIS3* gene with a flanking homology to *TPA1*. The *MAG1* and *REV3* genes were similarly replaced by *LEU2* and *TRP1* genes obtained from pRS305 and pRS304, respectively. Strains were grown at 30 °C in yeast extract peptone dextrose (YPD) or synthetic medium. All primer sequences are available upon request. A detailed list of the genotypes of the strains used in this study are also available upon request. The yeast strains were grown to early log phase (10^7 cells/ml) in the appropriate medium. For transformations with plasmids or PCR products, we used the standard lithium acetate-polyethylene glycol method.

Analysis of MMS Sensitivity—Sensitivity studies for S_N2 alkylating agents were performed with MMS. For the MMS sensitivity experiment by spot test, cells were grown in liquid YPD, washed, and suspended in water at a density of 1.5×10^7 cells/ml. Aliquots (7 μl) of the cell suspensions of different 10-fold dilutions were spotted onto solid YPD media containing various concentrations of MMS and grown at 30 °C for 3–5 days.

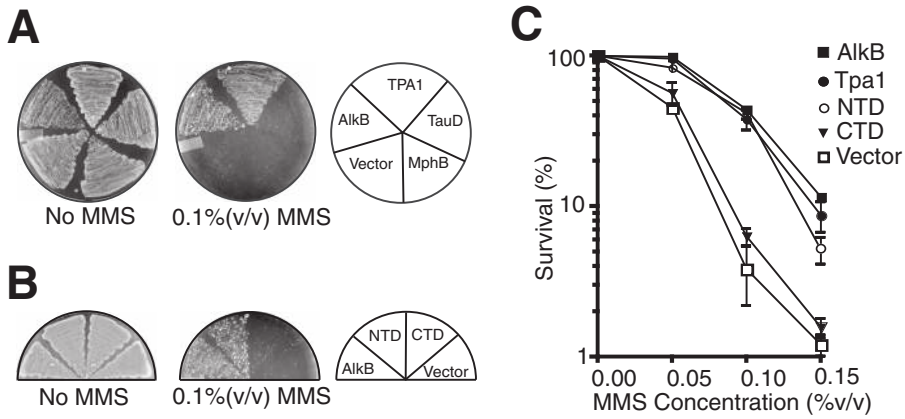

FIGURE 1. **Functional complementation of MMS sensitivity of the *E. coli alkB* strain HK82 by *S. cerevisiae* Tpa1.** *A*, MMS sensitivity of the *E. coli alkb*-deficient strain (HK82) expressing Tpa1, TauD, AlkB, MphB, and empty vector. *B*, MMS sensitivity of the *E. coli alkb*-deficient strain (HK82) expressing the Tpa1 NTD and CTD. Cells were treated with 0.1% (v/v) MMS for 3 h, plated on LB agar, and incubated at 37°C for 20 h. Survival was compared with cells expressing *E. coli* AlkB (positive control) and empty vector (pGex6p1, negative control). All strains were grown in duplicates. *C*, survival analysis of the *E. coli alkB* strain HK82-expressing *S. cerevisiae* Tpa1 constructs. Shown is a survival curve of the Tpa1-rescued *E. coli alkB* strain. *E. coli* strain HK82 (*alkB*) was transformed with different Tpa1 constructs and grown in cultures containing 0.05%, 0.1%, and 0.15% (v/v) of the methylating agent MMS for 2 h. Survival was determined by plating cells on LB agar at 37 °C for 20 h and colony counting. The viability of cells not treated with MMS was 100%. *Error bars* indicate mean ± S.E. All strains are isogenic derivatives of W303.

For survival analysis and quantification, cells were spread onto YPD plates with 0.5–1.5 μg/ml MMS and incubated at 30 °C, and then colonies were counted after 3–5 days.

Analysis of Sensitivity to Protein Synthesis Inhibitors—To study the effect of translational inhibitors, YPD plates supplemented with anisomycin (Sigma, catalog no. A9789), cycloheximide (Sigma, catalog no. 180179), geneticin (Himedia, catalog no. TC026), and paromomycin (Sigma, catalog no. P5057) were used. 6-Azauracil (Sigma, catalog no. A1757), 100 μg/ml, was used to assay the effect of the transcriptional inhibitor. Anisomycin was dissolved in dimethyl sulfoxide. Gentamicin and paromomycin stock solutions and YPD plates were prepared in 0.1 M KPO_4 buffer (pH 7.5). 10-Fold dilution spot assays to monitor the sensitivity to anisomycin (1.0 μg/ml), paromomycin (0.5 mg/ml), geneticin (80 μg/ml), 6-azauracil (100 μg/ml), and cycloheximide (0.03 μg/ml) were carried out as described previously (40).

RESULTS

Tpa1 Functionally Complements E. coli AlkB—Bacterial cells lacking AlkB are hypersensitive to exposure to S_N2 alkylating agents such as MMS (41). Furthermore, exponentially proliferating Alkb-deficient cells have been reported to be more sensitive to MMS than wild-type cells growing at a similar rate (42). We hypothesized that if *S. cerevisiae* Tpa1 were functionally similar to AlkB, then expression of Tpa1 would be able to suppress the MMS-sensitive phenotype of the *E. coli* alkB-deficient strain (HK82). To express the Tpa1 construct in *E. coli* HK82 strains, we cloned the Tpa1 gene in the pGex vector (GE Healthcare) directly downstream of the *lac* promoter and operator region so that the recombinant protein could be expressed without the requirement of T7 polymerase. Before complementation experiments were carried out, comparable expression levels in the HK82 strain from the different constructs were confirmed. We expressed *S. cerevisiae* Tpa1 and *E. coli* AlkB in HK82 cells and treated them with 0.01% (v/v) MMS for 2 h. Surprisingly, only the cells expressing Tpa1 and AlkB complemented the MMS-sensitive phenotype (Fig. 1*A*). Interestingly, the survival of Tpa1-expressing cells was similar to the cells expressing AlkB. However, cells expressing empty vector, as might be expected, completely lacked any complementation effect. To verify the specificity of Tpa1-mediated complementation, two more *E. coli* dioxygenases, the *mhpB* gene encoding catechol dioxygenase (43) and *tauD* encoding taurine hydroxylase (44), were cloned into the same vector and expressed in HK82 cells. As expected, these dioxygenases could not rescue the MMS sensitivity of the *alkB* mutant *E. coli* (Fig. 1*A*). The Tpa1 structure reveals the presence of two domains, the NTD, amino acids 1–268, and the CTD, amino acids 277–644. Although both of these domains are structurally similar, only the NTD has a conserved $HXDX_nH$ motif and binds iron and 2OG as in other Fe(II)/2OG-dependent dioxygenases (25). It would therefore be expected that only the NTD might retain the catalytic function and complement AlkB function. When we examined the ability of the NTD and CTD in suppressing the MMS-sensitive phenotype of *E. coli alkB* strain HK82, we observed that the NTD successfully complemented AlkB function but that the CTD could not, suggesting that the enzymatic activity of Tpa1 may be essential for complementing AlkB. We also analyzed complementation of *E. coli alkb* by Tpa1 at different concentrations of MMS (Fig. 1*C*). HK82 cells expressing different Tpa1 constructs were exposed to 0.05%, 0.1%, and 0.15% (v/v) MMS for 2 h, and cell survival was determined. The MMS sensitivity of *alkB* cells was reduced significantly when transformed with Tpa1 or the NTD, whereas cells expressing the CTD had only a small difference in sensitivity compared with the control vector (Fig. 1*C*). These observations strongly indicate that only the first 298 amino acids are necessary and sufficient for full complementation of the alkB mutant of *E. coli*. This indicates that the DNA repair activity is contained within this domain. The CTD may participate in unrelated functions or interactions with other proteins but is not necessary for the DNA repair activity itself. The protein has been claimed to

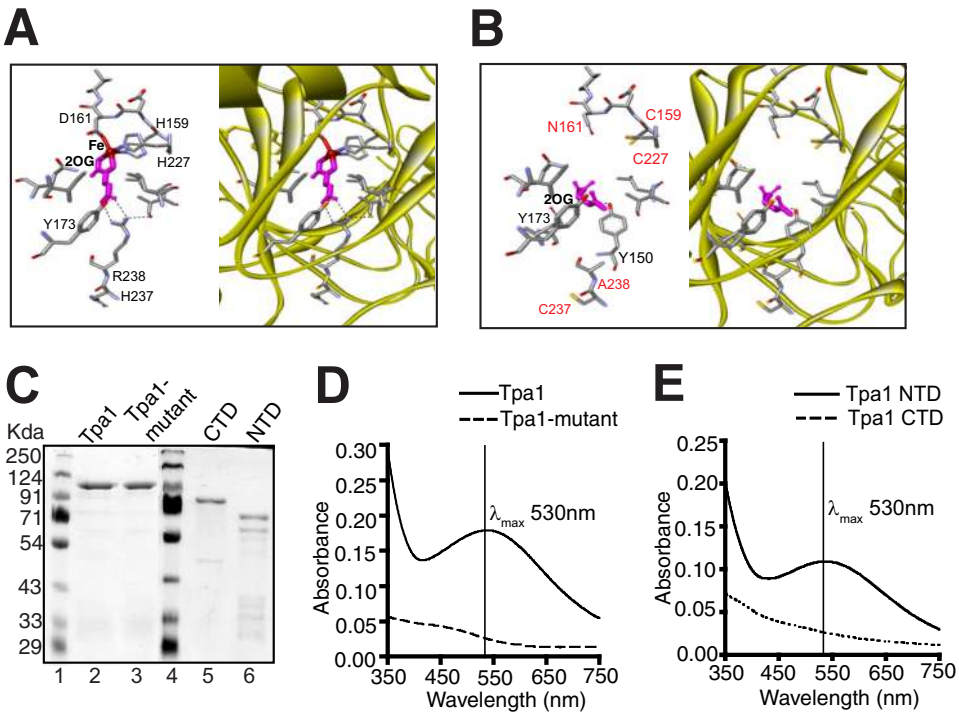

FIGURE 2. **Interaction of 2OG and iron with the active site residues of wild-type and mutant Tpa1.** *A*, crystal structures of the 2OG-bound Tpa1 (PDB code 3KT7). *B*, altered orientation and diminished atomic interactions of a representative position of docked 2OG bound to mutant Tpa1 (H159C, D161N, H227C, H237C, and R238A, *red*). *Ribbon representations* show the position of 2OG and iron with respect to the α helices and β strands of Tpa1. *Stick representations* depict the amino acids, and atomic bonds are represented by *dotted lines*. *C*, recombinant GST-AlkB, GST-Tpa1, GST-CTD, and GST-NTD were purified by glutathione-Sepharose and analyzed by 12% SDS-PAGE. *D*, UV-visible spectroscopic analysis showing evidence for binding of Fe(II) and 2OG by Tpa1 (*solid line*) and the Tpa1 mutant (*dotted line*). *E*, UV-visible spectra of Fe(II)-CTD (*dotted line*) and NTD (*solid line*). Peak absorption was recorded at 530 nm. Proteins were mixed with buffer containing 25 mM Tris-HCl (pH 8.0), 50 mM KCl, 0.5 mM 2OG, 4.0 mM sodium ascorbate, and 880 μM $FeSO_4$, and spectra were recorded.

function as a poly-A binding protein, and the CTD may contribute to such other unrelated activities, interactions with other repair proteins, or both (24, 25).

Design of a Tpa1 Mutation That Abolishes Cofactor Binding—The Tpa1 residues involved in binding to iron are His-159, Asp-161, and His-227 in the ternary structure of the Tpa1-Fe(III)-2OG complex (24, 25). Iron also coordinates with 2OG, which, in turn, interacts with and Ile-171, Tyr-173, Val-229, Arg-238, and Ser-240 (25). To generate a Tpa1 mutant, a molecular docking analysis was performed to confirm whether cofactor binding is indeed abolished using published structures of Tpa1 (24, 25) (Fig. 2*A*). On the basis of the Tpa1 structure and molecular docking analysis, we first introduced site-specific mutations of the conserved residues His-159, Asp-161, and His-227 to alanine and analyzed cofactor binding of this triple mutant by molecular docking. However, the mutant had little effect on iron and 2OG binding. Consequently, we decided to use the protein variation effect analyzer algorithm to predict amino acid substitutions that would result in significant functional differences (28). According to our molecular docking analysis, Tpa1 with H159C, D161N, H227C, H237C, and R238A mutations combined resulted in altered 2OG binding and concomitantly diminished iron binding (Fig. 2*B*). Next, we wanted to experimentally confirm the whether the Tpa1 mutation indeed resulted in loss of iron binding. We expressed recombinant Tpa1, the Tpa1 mutant, the NTD, and the CTD in *E. coli* and then purified by affinity chromatography to ~90% purity, as visualized via SDS-PAGE and Coomassie Brilliant Blue staining (Fig. 2*C*). Members of the Fe(II)/2OG-dependent dioxygenases forms chromophores associated with a metal-to-ligand charge transfer transition. When we monitored purified Tpa1 by UV-visible spectroscopy under the optimum conditions mentioned before (45), it generated the characteristic absorption peak at 530 nm when both metal and cofactor were present (Fig. 2*D*). This is in good agreement with the characteristic absorption peak of chromophores reported by others (33, 45, 46). However, the Tpa1-mutant, which lacks active site coordination of iron and 2OG, did not produce any spectrum associated with chromophore formation (Fig. 2*D*). This result is consistent with our observations from the molecular docking studies. An absorption peak at 530 nm was also observed when the NTD was analyzed (Fig. 2*E*). Interestingly, CTD absorption spectra in the presence of metal ion and cofactor revealed no characteristic absorption peak at 530 nm (Fig. 2*E*). On the basis of these observations and previous structural studies, it is clear that the Tpa1 mutant and the CTD lacked 2OG-bound iron in the catalytic site.

Tpa1 Catalyzes Methyl Base Lesion Repair—Because nothing is known about the DNA repair activity of Tpa1 protein, we used a simple *in vitro* repair assay using a synthetic 70-base oligonucleotide containing the methylation-sensitive restriction site MboI in the middle (35). The methylation-sensitive restriction enzyme MboI does not cleave methylated DNA substrate. The MMS-damaged oligonucleotide was directly incubated with Tpa1 for repair to take place, annealed with the complementary DNA to generate the double-stranded DNA,

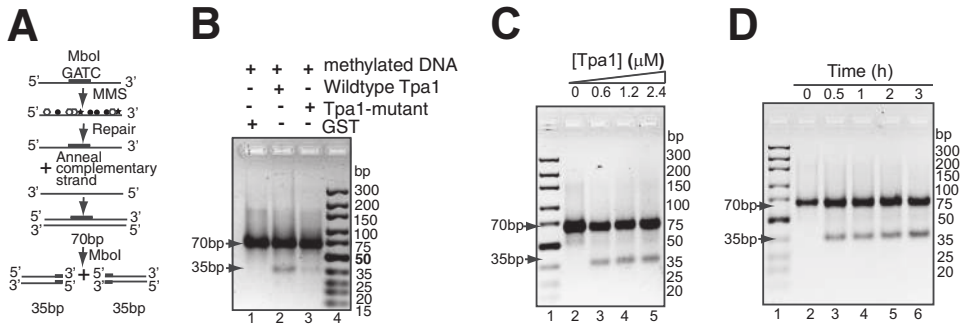

FIGURE 3. **Tpa1 is catalytically active and removes methyl adducts.** *A*, schematic of the restriction enzyme-based repair assay. A 70-bp oligonucleotide comprised of the recognition site for the methylation-sensitive restriction enzyme MboI (5′-GATC-3′) in the middle was treated with MMS. MMS-damaged oligonucleotides were incubated with Tpa1, and repaired DNA was annealed to a complimentary undamaged oligonucleotide and cleaved with the MboI restriction enzyme. *B*, Tpa1-catalyzed repair was detected by MboI digestion, followed by agarose gel electrophoresis and ethidium bromide staining. Tpa1, mutant Tpa1, and GST were incubated with methylated oligonucleotide. Following Tpa1-mediated repair, MboI digestion produced a 35-bp band, whereas MboI did not cleave mock-repaired (GST) and mutant Tpa1-repaired substrate, and the 70-bp substrate remained intact. The *arrows* indicate the positions of the 70- and 35-base pair bands. Single- and double-stranded DNA are represented as single-stranded DNA and dsDNA, respectively. *Lane 4* represents molecular size markers. *C*, increasing amounts of purified Tpa1 were added to methylated DNA substrate for 2 h at 30 °C, followed by MboI restriction analysis. Reactions were analyzed by agarose gel analysis as mentioned before. *D*, time course of Tpa1 repair. Tpa1 was added to methylated DNA substrate for 0.5, 1, 2, and 3 h at 30 °C, followed by MboI restriction analysis. Reactions were analyzed by agarose gel analysis as mentioned before.

analyzed on 3% agarose gel using 10 mM sodium borate as electrophoresis buffer, and stained with ethidium bromide (Fig. 3*A*). We observed that Tpa1 could repair methylated DNA, as evident from the appearance of a 35-bp band (Fig. 3*B*, *lane 2*). This result is consistent with our observation that Tpa1 forms characteristic chromophores in the presence of metal ion and cofactor (Fig. 2*E*). We also observed previously that the Tpa1 mutant failed to form a complex with iron and 2OG (Fig. 2*E*). To investigate whether direct repair of MMS-damaged DNA is abrogated in the mutant lacking cofactor binding, we analyzed Tpa1 mutant-treated samples with MboI digestion. Interestingly, no MboI-cleavable band was formed in the presence of the Tpa1 mutant with single-stranded DNA (Fig. 3*B*, *lane 3*), suggesting that there was no DNA repair activity present in the Tpa1 mutant. These results establish that Tpa1 is catalytically active and that it depends on Fe(II) and 2OG binding for its activity.

To confirm the specificity of this reaction, we analyzed the effect of increasing concentrations of Tpa1 (0.6–2.4 μM). As shown in Fig. 3*C*, *lanes 2–5*, we observed a gradual increase of the 35-bp band, both in the case of double and single-stranded DNA. These data, in agreement with earlier observations, showed that products with fewer numbers of methylated base lesions can be obtained using high enzyme concentrations. Longer incubation with Tpa1 also resulted increased amounts of product DNA free of methylated base lesions, as detected by MboI cleavage, both in the case of double- and single-stranded DNA (Fig. 3*D*, *lanes 2–6*). However, our assay detected repair by restoration of MboI restriction site and depended on the specificity of the restriction enzyme, unlike the conventional HPLC-based assay, which directly measures demethylation by retention of methylated nucleotides in DNA. Therefore, this approach could not confirm which lesions are recognized and repaired by Tpa1 protein because the nature of the MboI digestion-inhibiting lesions was unknown. Nonetheless, this simple assay was sufficient to demonstrate that Tpa1 is catalytically active and able to carry out repair of methylated nucleotides that can restore DNA into a form that can be cut by MboI.

Tpa1 Repairs MMS-damaged DNA by Oxidative Demethylation—The hallmark of AlkB-mediated oxidative demethylation is that the oxidized methyl group is removed as formaldehyde. Hydroxylation of the methyl group is followed by spontaneous release of the resulting hydroxymethyl moiety as formaldehyde (13, 47). Therefore, it would be expected that Tpa1 would catalyze the conversion of methyl adducts that is spontaneously released as formaldehyde, regenerating the normal bases. To test whether formaldehyde is released during the Tpa1-mediated DNA repair reaction, we used two different assay methods.

First, we used direct fluorescence-based formaldehyde detection using acetoacetanilide. Acetoacetanilide reacts with formaldehyde and forms a fluorescent dihydropyridine derivative with peak emission at 465 nm. We generated a standard plot using a series of dilutions (0.1–50 μM) of formaldehyde (Fig. 4*A*). Various concentrations of formaldehyde (50 μl) were added to ammonium acetate (40 μl) and acetoacetanilide (10 μl) in a 100-μl reaction. On the basis of an emission peak at 465 nm (Fig. 4*A*), a linear relationship was observed between the concentration of formaldehyde and the fluorescence of the reaction product (Fig. 4*B*). We found that the detection limit of this assay was 0.5 μM. After confirming that the acetoacetanilide and formaldehyde reaction product could be detected by fluorescent spectrometry, we wanted to know whether demethylation repair activity of Tpa1 could also be detected by the presence of formaldehyde. To carry out the *in vitro* DNA repair reaction, purified recombinant proteins were used. *E. coli* AlkB was used as a positive control. Following the repair reaction, acetoacetanilide and ammonia were added directly to the reaction mix. We noticed distinct emission spectra with a peak emission of 465 nm when *E. coli* AlkB or *S. cerevisiae* Tpa1 was present (Fig. 4*C*). Because we had already established that formaldehyde reacts with ammonia and acetoacetanilide to form a fluorescent compound with a peak emission of 465 nm, this result proved the formation of formaldehyde as a result of the removal of methyl adducts (Fig. 4*C*). Notably, 2 μM of AlkB and Tpa1 resulted in a similar amount of formaldehyde release,

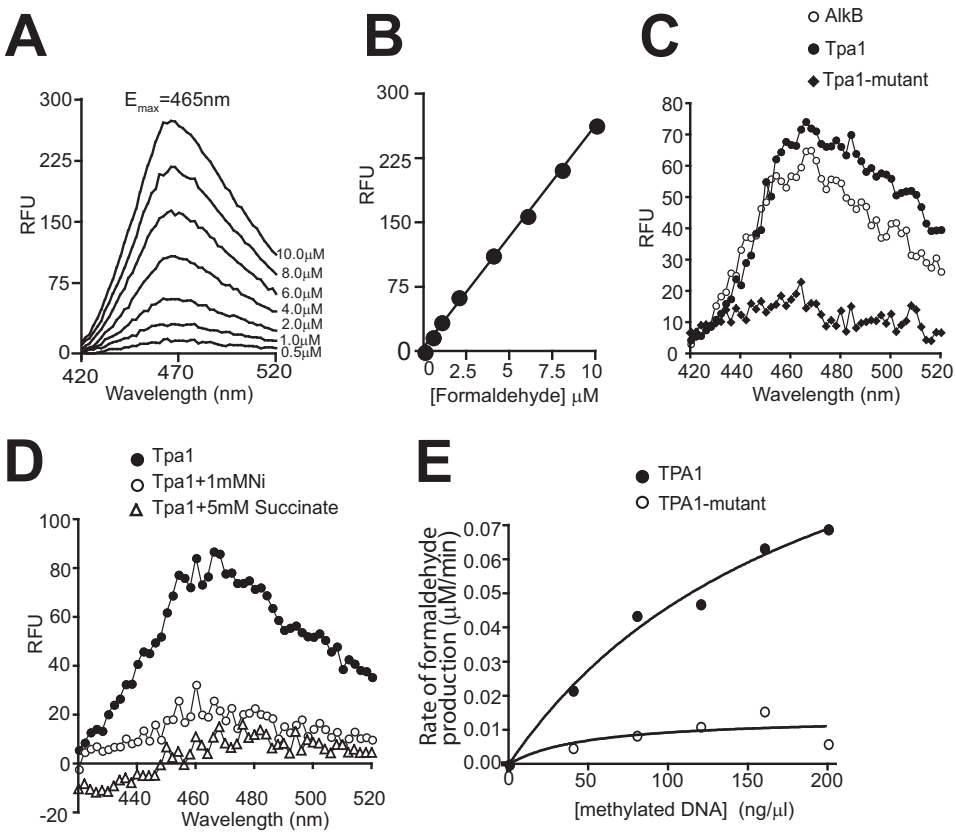

FIGURE 4. **Tpa1 is involved in direct repair of methylated DNA.** *A*, emission spectra of the product of reaction between ammonia and acetoacetanilide and different concentrations of formaldehyde. *B*, standard plot of absorbance *versus* different concentrations of formaldehyde. *C*, emission spectra of the product of reaction between ammonia, acetoacetanilide, and a sample containing either AlkB or Tpa1 or mutant-Tpa1-repaired methylated DNA. The repair reaction was carried out with a fixed amount (2 μM) of bacterially expressed and purified recombinant protein (GST-Tpa1, GST-Tpa1-mutant, and GST-AlkB) and MMS-damaged single-stranded DNA substrate (100 ng/μl) at 30 °C for 1 h. A sample containing 2 μM GST and MMS-damaged single-stranded DNA (100 ng/μl) was used as background fluorescence correction. *D*, emission spectra of the product of reaction between ammonia, acetoacetanilide, and a sample containing Tpa1 in the presence of divalent nickel ion and the competitive inhibitor succinate. The reaction components were the same assays as in *C*, except 1 mM Ni(II) or 5 mM succinate was present. *E*, bacterially expressed and purified Tpa1 and Tpa1-mutant proteins were incubated with MMS-damaged single-stranded DNA substrate of different concentrations. DNA repair activity was monitored by quantifying formaldehyde release as mentioned in *C* and plotted. Graphs represent averages of triplicate experiments. Curve fitting was carried out using GraphPad Prism software.

as detected by the formation of a fluorescent dihydropyridine product, suggesting equal repair efficiency. Next, we decided to test whether the Tpa1 mutation that affects iron and 2OG binding to the active site has a reduced DNA repair activity. As expected, mutation of the residues involved in iron and 2OG binding resulted in diminished DNA repair activity (Fig. 4*C*). However, the mutant Tpa1 still retained some marginal activity. We speculate that this could be due to low-level background activity contributed by the Tpa1 CTD that contains a conserved double strand β-helix fold found in all AlkB homologs.

Prior studies have shown that Fe(II)/2OG-dependent oxygenases are sensitive to inhibition by divalent transition metal ions (48). To test whether Tpa1 is also inhibited similarly, we analyzed the effect of nickel ion by incubating Tpa1 with 1 mM nickel ions. We found that nickel ion strongly inhibited the demethylase activity of Tpa1 (Fig. 4*D*). Fe(II)/2OG-dependent oxygenases are also known to be competitively inhibited by compounds structurally similar to 2-oxoglutarate, *e.g.* succinate (49). As shown in Fig. 4*D*, 5 mM succinate strongly inhibited demethylase activity of Tpa1. These results clearly indicate that the mechanism of inhibition of Tpa1 activity is very similar to other Fe(II)/2OG-dependent oxygenases.

To test whether the repair-associated formaldehyde release is affected in the Tpa1 mutant, methylated DNA substrate was increased from 40–200 ng/μl, keeping the amount of Tpa1 (2 μM) or Tpa1 mutant constant. We observed a proportional increase in the formaldehyde production in the Tpa1-mediated reaction (Fig. 4*E*). However, repair-associated formaldehyde release was diminished in Tpa1 mutant. This result confirmed that mutation of the cofactor binding residues affected Tpa1 activity (Fig. 4*E*). Together, these data suggest that Tpa1 has DNA repair activity and specifically removes methyl adducts as formaldehyde.

To further confirm that formaldehyde was indeed generated in the Tpa1-mediated demethylation reaction, we used an alternate indirect assay method. FDH converts formaldehyde to formate using NAD^+ as the electron acceptor whose reduction to NADH can be spectrophotometrically measured from absorbance at 340 nm (Fig. 5*A*). Such an indirect assay is routinely used to monitor enzymatic reactions involving formaldehyde release, *viz.* JmjC histone demethylase-catalyzed reactions (50). In the FDH-coupled demethylation assay, we determined the DNA repair activity of Tpa1 by measuring the production of NADH. A standard curve that was first generated using 0.01

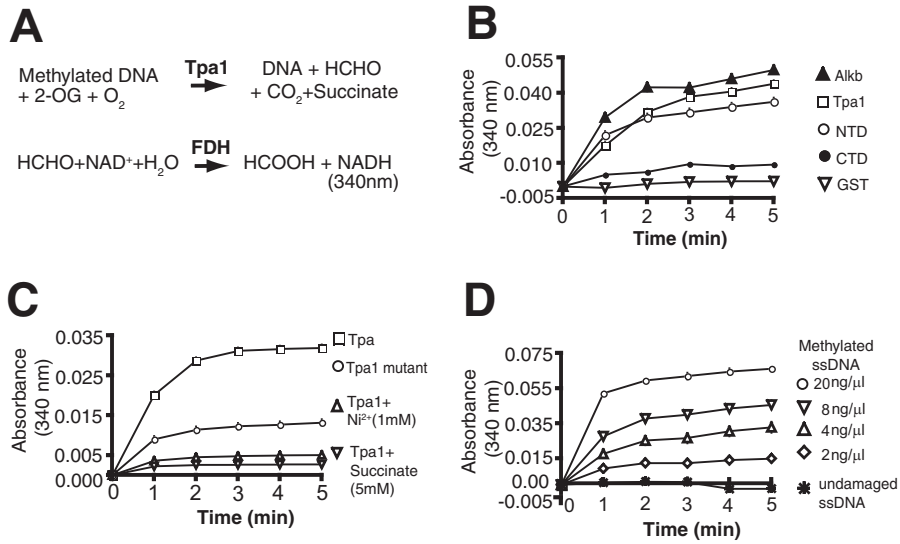

FIGURE 5. **FDH-coupled assay to detect formaldehyde produced during Tpa1-mediated repair.** *A*, chemical reaction for formaldehyde production and its detection by FDH-coupled assay. *B*, demethylation reaction using purified GST-fused recombinant proteins (2 μM), *viz.* Tpa1, Tpa1-NTD, Tpa1-CTD, AlkB, and MMS-damaged single-stranded DNA substrate (10 ng/μl). The repair reaction was coupled to the FDH reaction by adding 0.01 units of FDH and 1 mM NAD^+. The reaction was monitored continuously for the production of NADH (absorption at 340 nm). *C*, direct reversal of methylated DNA as revealed by formaldehyde release by wild-type Tpa1 but not with a Tpa1 mutant that lacks cofactor binding. Reactions in the presence of divalent nickel ion and the competitive inhibitor succinate were the same assays as in *B* but contained 1 mM Ni(II) or 5 mM succinate. *D*, FDH-coupled demethylation assays with a fixed amount (2 μM) of Tpa1 and varying amounts (2–20 ng/μl) of the MMS-damaged single-stranded DNA (*ssDNA*) substrate. Undamaged single-stranded DNA was used as a negative control.

units of FPLC-purified FDH, 1 mM NAD^+, and different amounts of formaldehyde. Within the range of 5–50 μM formaldehyde, a linear relationship was found between the production of NADH and the amount of formaldehyde used. Subsequently, the FDH-coupled demethylation assays were carried out within this linear range. The reactions were initiated by adding the MMS-damaged single-stranded DNA as substrate. As the demethylation proceeded, measuring absorbance at 340 nm at different time points revealed the production of formaldehyde. As shown in Fig. 5*B*, within the first 2 min of the reaction, a robust increase of absorbance at 340 nm was observed, indicating that substantial amounts of formaldehyde were produced in the Tpa1-catalyzed demethylation reaction. The fact that formaldehyde was generated in the demethylation reaction of damaged DNA strongly suggests that the reaction had occurred as proposed in Fig. 4*A*. As a positive control we used purified recombinant *E. coli* AlkB, and we detected a formaldehyde release comparable with Tpa1, suggesting that Tpa1 and AlkB have a similar ability to demethylate MMS-modified single-stranded DNA. Furthermore, only when MMS-damaged DNA was incubated with Tpa1, but not GST, did we detected a robust increase in the absorbance at 340 nm, indicating that the production of formaldehyde is specific for Tpa1 and a result of successful demethylation (Fig. 5*B*). Next, we wanted to confirm the effects of the Tpa1 mutation on iron and 2OG binding to the active site. As expected, mutant Tpa1 had diminished DNA repair activity (Fig. 5*B*). An FDH-coupled Tpa1-mediated repair assay also proved that 1 mM nickel ion and 5 mM succinate strongly inhibited the demethylase activity of Tpa1 (Fig. 5*C*). We next turned to using the FDH-coupled AlkB assay to investigate the specificity of the Tpa1 reaction. By keeping the amount of Tpa1 (1 μM) constant when methylated DNA was increased from 2–20 ng/μl, a proportional increase in the formaldehyde production was observed (Fig. 5*D*). Formaldehyde release was observed only when MMS-damaged DNA was used. In the presence of undamaged DNA, formaldehyde release was not detected. Together, the data from the indirect FDH-coupled repair assay supported our observations from the direct repair assay.

Collectively, the results from the direct and indirect formaldehyde detection assays strongly indicate that budding yeast Tpa1, like bacterial AlkB, could directly convert methyl adduct to an unstable hydroxymethyl product that is spontaneously released as formaldehyde.

Genetic Interaction of tpa1 with the DNA Glycosylase Mutant mag1—To better understand the role of Tpa1 *in vivo* in the context of DNA damage response, we analyzed the sensitivity of the *tpa1*Δ mutant to the DNA-alkylating agent MMS by spot test and survival assays. Survival or recovery assays unveil the nature of genetic interactions by scoring whether double mutants show epistatic, additive, or synergistic effects for survival or recovery. We observed that the *tpa1*Δ mutant was not very sensitive to chronic exposure to MMS at lower concentration and only modestly MMS-sensitive at a higher concentration (Fig. 6*A*). Interestingly, the *tpa1*Δ strain has indeed been reported as mildly MMS-sensitive in a genetic screen (27).

These results prompted us to examine whether there is any redundancy in the repair of methylated bases by the 3meA-specific DNA glycosylase Mag1. As shown in Fig. 6*A*, deletion of *MAG1* results in modest MMS sensitivity at a higher concentration of MMS, and this is consistent with an earlier report (51). However, when *tpa1*Δ was combined with the deletion of the DNA glycosylase Mag1, the double mutant *tpa1*Δ*mag1*Δ was significantly more sensitive to MMS than the individual single mutant (Fig. 6*B*). These results suggest that there is an overlap of function (synergism) between Mag1-initiated BER

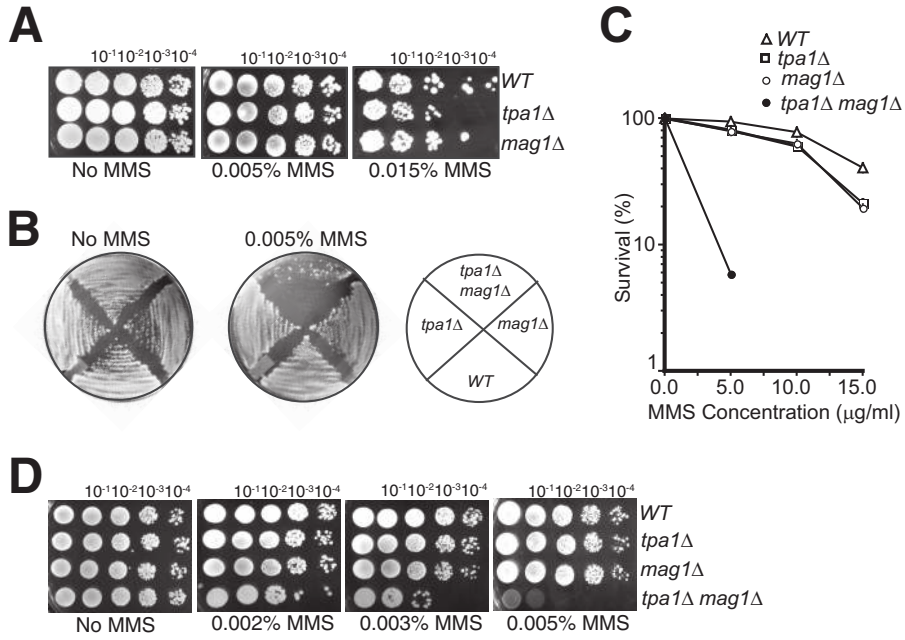

FIGURE 6. **Effect of the deletion of Tpa1 and the BER pathway DNA glycosylase Mag1 on cell viability during MMS treatment.** *A*, mildly MMS-sensitive phenotypes of the *tpa1*Δ and *mag1*Δ mutants. 10-fold dilutions of log-phase cultures of the wild-type strain (W303) and the *mag1*Δ and *tpa1*Δ strains were spotted on YPD supplemented with increasing concentrations (0.005% and 0.015% (v/v)) of MMS. *B*, hypersensitivity of the *tpa1*Δ *mag1*Δ double mutant strain to MMS-induced DNA damage compared with *tpa1*Δ and *mag1*Δ. Colonies of each strain were streaked onto a YPD plate containing either no MMS or 0.005% (v/v) MMS. As a control, the wild-type strain (W303) was streaked. Plates were incubated at 30 °C for 3 days and then photographed. *C*, the effect of MMS on the viable cell population of the *S. cerevisiae* wild-type strain (W303), *mag1*Δ, *tpa1*Δ, and the *mag1*Δ*tpa1*Δ double mutant. Cells were spread onto MMS-containing YPD plates and incubated at 30 °C, and then colonies were counted after 3–5 days. Graphs represent averages of four experiments. *D*, MMS-sensitive phenotypes of the *tpa1*Δ*mag1*Δ double mutant. 10-fold dilutions of log-phase cultures of the *tpa1*Δ, *mag1*Δ, and *tpa1*Δ*mag1*Δ strains were exposed to increasing concentrations (0.002%, 0.003%, and 0.005% (v/v)) of MMS on YPD plates and incubated at 30 °C for 3 days. Representative images of repeat experiments are shown.

and direct repair mediated by Tpa1 for the repair of alkylation damage. To quantify MMS sensitivity of the single and double mutants, survival was monitored by scoring colony growth on media containing different concentration of MMS.

When exposed to methylation damage, cells lacking either *MAG1* or *TPA1* expression showed susceptibility to methylation-induced toxicity. However, the susceptibility to MMS-induced methylation damage was increased significantly in double mutant cells (Fig. 6*C*). Loss of Tpa1 and Mag1 alone affected survival but to a lesser extent than the *mag*Δ*1tpa1*Δ double mutation because no survivors were recovered on 1 μg/ml MMS in the double mutants (Fig. 6*C*). In *S. cerevisiae*, Mag1 is known to remove 3meA. Our observation that *mag*Δ*1tpa1*Δ double mutants are synergistically more susceptible to methylation damage hints at overlapping substrate specificity of Mag1 glycosylase and Tpa1 dioxygenase. Given the remarkable ability of 3meA to stall replication, it would not be surprising if the two different repair pathways have evolved to provide cell survival.

*MMS Sensitivity of the mag1*Δ*tpa1*Δ *Double Mutant Strain Is Not Due to Defective Protein Translation*—Increased sensitivity to the alkylation agent MMS has also been reported to arise when a deficiency of proteins involved in the BER pathway is combined in the protein modification pathway (52). In other words, if Tpa1 were involved in the regulation of protein synthesis, then the *mag1*Δ*tpa1*Δ double mutant would show increased sensitivity to MMS. Sensitivity to paromomycin, hygromycin, anisomycin, and geneticin aminoglycoside antibiotics decrease the translational accuracy by stimulating the stable association of aminoacyl tRNA to the ribosomal A site (53). Hypersensitivity of the mutant strain toward these antibiotics, especially paromomycin, has often been linked to loss of translational accuracy or incorrect decoding of the mRNA (54). We hypothesized that if MMS sensitivity of *mag1*Δ *tpa1*Δ were due to any role of Tpa1 in translational accuracy, then *mag1*Δ *tpa1*Δ would be sensitive to these antibiotics. Accordingly, we analyzed the sensitivity of the *tpa1*Δ, *mag1*Δ, and *mag1*Δ*tpa1*Δ double mutants to each of these antibiotics by spot test (Fig. 7). We also included a strain deficient in Stp22 in the study as a positive control. It has been reported that *stp22*Δ cells are sensitive to these antibiotics because it is a component of the endosomal sorting complexes required for transport (ESCRT) complex that is involved in ubiquitin-dependent sorting of proteins into the endosome (52). As shown in Fig. 7, paromomycin, hygromycin, anisomycin, and geneticin did not show any effect on the *tpa1*Δ, *mag1*Δ, and *mag1*Δ*tpa1*Δ double mutants. These results suggest that deletion of Tpa along with Mag1 does not lead to any defect in translation elongation. Resistance to paromomycin also indicates that *tpa1* single and *mag1*Δ*tpa1*Δ double mutants are not defective with respect to fidelity of protein synthesis. Additionally, we tested the sensitivity to the general translation inhibitor cycloheximide and the transcription inhibitor 6-azauracil, a drug that promotes transcriptional stalling by lowering GTP concentrations (Fig. 7). Standard 10-fold dilution spot assays revealed that the *tpa1*Δ, *mag1*Δ, and *mag1*Δ*tpa1*Δ double mutants were also not sensitive to the translation inhibitor cycloheximide or the transcription inhibitor 6-azauracil (Fig. 7), suggesting that these mutants do not

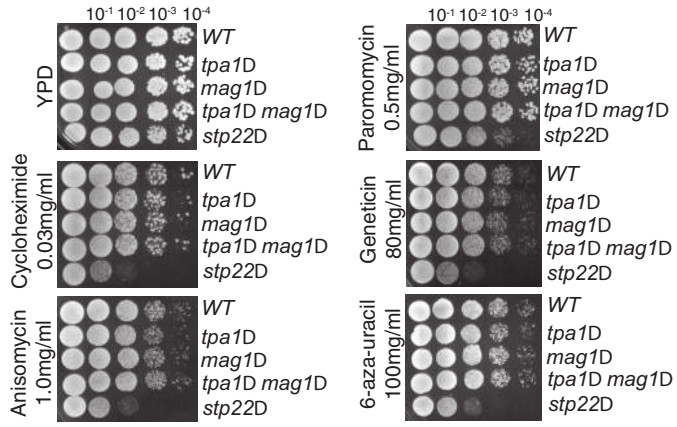

FIGURE 7. **Effect of deletion of Tpa1 and Mag1 on cell viability during treatment with translational inhibitors.** 10-fold dilutions of cells harboring the indicated mutations were spotted onto YPD medium containing the indicated concentrations of cycloheximide, anisomycin, paromomycin, geneticin, and 6-azauracil. Cells were incubated for 3 days at 30 °C, and growth was monitored compared with growth on plates in the absence of drug. Each strain and drug was assayed at least three times.

have any general protein synthesis defect. From these findings it is clear that the MMS sensitivity of the *mag1*Δ*tpa1*Δ double mutant could possibly be due to incomplete DNA repair and not due to a lack of translational accuracy.

Genetic Interaction of tpa1 with Error-prone DNA Polymerase Mutants—We observed that, although the *mag1*Δ*tpa1*Δ double mutant was sensitive to MMS, it could tolerate lower doses of MMS (Fig. 6*D*). To investigate how *mag1*Δ*tpa1*Δ double mutant cells are surviving a low level of MMS-induced damage, we hypothesized that, in *mag1*Δ*tpa1*Δ cells, damage bypass replication might contribute to cell survival. In budding yeast, damage bypass replication is carried out by any of the three TLS polymerases: Polη (Rad30), Polζ (Rev3, Rev7), and Rev1. To assess the role of TLS polymerases, we combined deletion of *MAG1* or *TPA1* with those of *RAD30* (Polη), *REV3* (Polζ), or *REV1* polymerases. We observed that only *mag1*Δ*rev3*Δ and *tpa1*Δ*rev3*Δ showed MMS sensitivity (Fig. 8, *A* and *B*). None of the other TLS polymerase double mutants (*mag1*Δ*rad30*Δ, *mag1*Δ*rev1*Δ and *tpa1*Δ*rad30*Δ, *tpa1*Δ*rev1*Δ) displayed increased susceptibility to MMS than the single mutant *mag1*Δ or *tpa1*Δ (Fig. 8*C*). These results suggest that, among the TLS polymerases, lack of *REV3* (Polζ) expression alone renders *tpa1*Δ or *mag1*Δ cells susceptible to methylation damage. This is not surprising because Polη (*RAD30*) is involved in error-free replication of UV-induced cyclobutane-pyrimidine dimer-specific damage. Pol ζ, in contrast, participates in error-prone TLS across lesions produced by a variety of DNA-damaging agents, including MMS. Therefore, lack of Pol ζ, combined with lack of Tpa1 or Mag1, displays such a strong synergistic effect (Fig. 8, *A* and *B*). Together, these results provide strong evidence to suggest that Polζ (Rev3) is probably the TLS polymerase that contributes to cell survival in the presence of MMS-damaged DNA. Interestingly, both the *mag1*Δ*rev3*Δ and *tpa1*Δ*rev3*Δ double mutants were less sensitive to MMS than the *tpa1*Δ*mag1*Δ double mutant (Fig. 8, *A* and *B*). The double mutants *mag1*Δ*rev3*Δ and *tpa1*Δ*rev3*Δ had functional Tpa1 and Mag1, respectively. Therefore, this genetic interaction apparently indicates that the damage bypass polymerase Polζ may possibly be functionally secondary and less preferred by cells than Mag1 and Tpa1 in dealing with MMS-damaged DNA.

Further, we sought to determine whether removing the Polζ function in the *mag1*Δ*tpa1*Δ double mutant strain would completely abolish the entire cellular defense mechanism against DNA alkylation damage. As shown in Fig. 6, *D* and *E*, survival of the *tpa1*Δ*mag1*Δ*rev3*Δ triple mutant was reduced dramatically compared with the *tpa1*Δ*mag1*Δ double mutant and displayed a sensitivity to lower concentrations of MMS. These genetic interactions establish a connection between Tpa1 activity, the alkyl base DNA glycosylase Mag1, and error-prone DNA polymerase Polζ and confirm that, indeed, Tpa1 has an important role in overall cellular defense against DNA alkylation damage.

DISCUSSION

This work comprises the first report of existence of direct alkylation damage reversal pathway apart from Mgt1 in *S. cerevisiae* and identification of Tpa1 as the functional homolog of *E. coli* AlkB. Since the discovery AlkB decades ago, the budding yeast homolog has remained elusive. To our knowledge, no DNA repair function has been attributed to the Tpa1 protein so far. We provide evidence that not only establishes *S. cerevisiae* Tpa1 as a Fe(II)/2OG-dependent dioxygenase but also unravels that Tpa1 acts synergistically with the BER pathway against the S_N2-type alkylating agents. We also establish that the synergistic MMS-sensitivity phenotype is not due to defective protein synthesis.

Rescue of the Alkylation-sensitive Phenotype of the E. coli alkB Mutant—Because DNA alkylation repair pathways are highly conserved between prokaryotes and eukaryotes, we speculated that AlkB homolog(s) might also exist in *S. cerevisiae*. The only protein with significant amino acid sequence homology and structural similarity to the Fe(II)/2OG-dependent oxidative demethylases, including *E. coli* AlkB protein, is Tpa1 (22). Tpa1 has been considered to be a prolylhydroxylase (24, 26). To test the idea that Tpa1 could be the functional homolog of AlkB more rigorously, we sought to examine whether expression of Tpa1 in the *alkB* mutant *E. coli* strain could suppress the MMS sensitivity. Remarkably, full-length Tpa1 as well as the NTD rescued MMS hypersensitivity of *alkB* mutant (HK82) cells (Fig. 1). Only two human homologs of AlkB with DNA repair activity, hALKBH2 and hALKBH3, also showed a similar suppression of MMS hypersensitivity of *alkB* mutant (HK82) cells (14, 55). Importantly, the CTD, which lacked conserved catalytic residues, failed to provide protection against MMS (Figs. 1 and 2), indicating that, between the two domains, the Tpa1 NTD may be functionally active. Taken together, these observations made a strong case for Tpa1 being a functional homolog of *E. coli* AlkB.

In Vitro Oxidative Demethylation—Fe(II)/2OG-dependent dioxygenases display spectral properties associated with metal-to-ligand charge transfer transition in the presence of iron. Although Tpa1 has been characterized before (24–26), this spectroscopic characteristic was not known in Tpa1. We added excess Fe(II) and 2OG to recombinant Tpa1 and observed an UV-visible band with peak absorption at 530 nm for the native protein, as described previously (33, 45, 46). This is the first

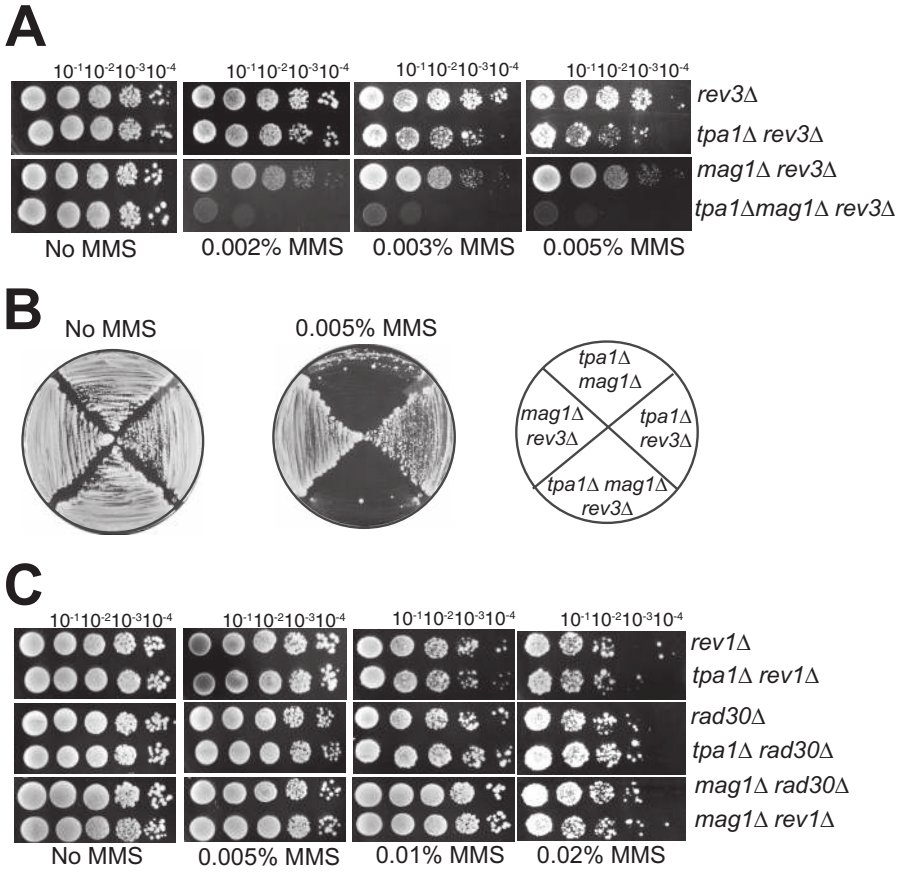

FIGURE 8. **Effect of the deletion of Tpa1, Mag1, and TLS DNA polymerases Polζ (Rev3) on cell viability during MMS treatment.** *A*, MMS-sensitive phenotypes of the *tpa1Δmag1Δrev3Δ* triple mutant. 10-fold dilutions of log-phase cultures of the *mag1Δrev3Δ*, *tpa1Δrev3Δ*, and *tpa1Δmag1Δrev3Δ* strains were exposed to increasing concentrations (0.002%, 0.003%, and 0.005% (v/v)) of MMS on YPD plates and incubated at 30 °C for 3 days. Representative images of repeat experiments are shown. *B*, MMS sensitivity of the *tpa1Δ mag1Δ rev3Δ* triple mutant strain compared with the *tpa1Δmag1Δ*, *tpa1Δrev3Δ*, and *mag1Δrev3Δ* double mutant strains. Colonies of each strains were streaked onto a YPD plate containing either no MMS or 0.005% (v/v) MMS. Strains were grown as before. *C*, MMS sensitivity of strains lacking the TLS polymerases Polη (Rad30) and Rev1. 10-fold dilutions of log-phase cultures of the *rev1Δ*, *rad30Δ*, *mag1Δrad30Δ*, *tpa1Δrad30Δ*, *mag1Δrev1Δ*, and *tpa1Δrev1Δ* strains were exposed to increasing concentrations (0.005%, 0.01% and 0.02% (v/v)) of MMS on YPD plates and incubated at 30 °C for 3 days. Representative images of repeat experiments are shown.

evidence of a metal-to-ligand charge transfer transition in Tpa1, clearly indicating a catalytic function.

Among the human AlkB homologs, hALKBH3 and hALKBH2 conclusively showed DNA repair activity (56). Using highly purified recombinant protein, we demonstrated that Tpa1 could demethylate single- and double-stranded DNA (Fig. 3). This enzymatic activity implies that Tpa1 may have a role in the maintenance of global genomic DNA as well as nuclear single-stranded DNA, found during cellular events like transcription. The human genome codes for at least nine AlkB homologs, and it seems rather likely that theses homologs functionally complement each other. Therefore, it was tempting to speculate Tpa1 may possess some of the functions of these homologs. Using single-stranded DNA as a substrate, Tpa1 activity was found to be very similar to AlkB (Fig. 5*B*). Iron and 2OG binding to the active site of Tpa1 was found to be crucial for activity because mutant Tpa1, which lacked iron-coordinating residues, failed to repair DNA (Figs. 3–5). Finally, Fe(II)/2OG-dependent dioxygenases, including AlkB, have been known to be strongly inhibited by divalent transition metal cations and competitively inhibited by succinate (48, 49). All of these phenomena were also observed here with Tpa1 (Figs. 4 and 5). Overall, these *in vitro* assays unambiguously establish Tpa1 as a Fe(II)/2OG-dependent oxidative demethylase specific to restoring MMS-damaged DNA. Our analysis of the mutant Tpa1 revealed that often DNA repair-related proteins are associated with chromatin. Indeed, previous studies have shown that Tpa1 is associated with yeast chromatin and copurified with the histone acetyltransferase complex NuA3 (57, 58). Future studies of Tpa1 should focus on the recruitment and activity of Tpa1 in the context of chromatin and how this might be regulated.

Further Insights into the Collaboration between DNA Repair Pathways Obtained from Genetic Interactions of Tpa1—The genetic interactions between alkylation-specific demethylase and glycosylase in *S. cerevisiae* was revealed for the first time in this study. This not only offered a qualitative assessment of repair dynamics but also allowed the analysis of pathway-dependent effects in eukaryotes. Although observed previously in *E. coli* (59), the interdependence of alkylation-specific demethylase and glycosylase in protecting cells from MMS-induced damage that we unveil here was hitherto unknown in eukaryotes. A significant overlap of function between Mag1 and Tpa1 also causes a lack of susceptibility to sublethal doses of

MMS in *tpa1*Δ cells (Fig. 6*A*). This also explains the question of why *mag1*Δ cells are also not particularly susceptible to sublethal dose of MMS (60, 61). It is possible that it is due to this reason that Tpa1 was never identified before as an obvious candidate gene associated with DNA repair in genetic screens (27, 62). Our analysis also revealed that, in the absence of Rev3 (Polζ), Tpa1 and Mag1 contribute equally to DNA alkylation repair. Surprisingly, Polζ could compensate in the absence of either Tpa1 or Mag1 when the other one is present. However, when both Mag1 and Tpa1 were deleted and only Polζ was present, it could not substitute for the roles of both Tpa1 and Mag1.

It is very difficult to imagine that mammalian Polζ would be able to compensate for the loss of both 3meA-specific DNA glycosylases and oxidative demethylase. For example, when the mammalian *alkA* homolog Aag was mutated along with two functional *alkB* homologs (hALKBH2 and hALKBH3), such $Aag^{-/-}Abh2^{-/-}Abh3^{-/-}$ triple knockout mice did not exhibit a significantly increased susceptibility to the alkylating agent MMS compared with $Aag^{-/-}$ single knockout mice (63). However, this does not necessarily mean that cells were actually protected from MMS-induced damage by mammalian Polζ. Because the mammalian genome codes for nine AlkB homologs, this could also be due to the presence of other active AlkB homologs. For example, weak AlkB-like repair activities have also been shown for hALKBH1 and fat mass and obesity associated *in vitro* (17, 30). Nonetheless, Polζ, and perhaps Polι and Polκ, may also have important roles in promoting replication through the 3meA adduct (5). It is also difficult to address the role of either DNA glycosylases or oxidative demethylases in the absence of the mammalian TLS polymerase Polζ. This is because $Rev3^{-/-}$ knockout has been reported as embryonic lethal and because $Rev3^{-/-}$ cell lines could not be established (64). By contrast, we clearly show that, in *S. cerevisiae* in the absence of either Mag1 or the AlkB homolog Tpa1, error-prone repair by Polζ supports cell survival (Fig. 5, *D* and *E*). Therefore, this rather simple yeast system may help to decipher the complex network of alkylation damage repair pathways in other eukaryotes.

Relevance of the Genetic Interaction between Alkyl Base Glycosylase and Oxidative DNA Demethylase to Cancer Therapy—The study of the genetic interaction among 3meA-specific DNA glycosylases, oxidative demethylases, and trans-lesion DNA polymerases is particularly important in view of its potential role in determining the efficacy and specificity of cancer therapy. If the same DNA repair deficiencies that sensitize tumor cells to chemotherapy or radiotherapy also allow them to continue replicating regardless of damage and, simultaneously, reduce their efficiency of DNA repair, then any DNA-damaging therapy could carry a risk of allowing further deleterious mutations to accumulate in any tumor cells that survive the treatment. Therefore, it is important to consider the actual DNA repair pathway operating in response to particular forms of damage in particular tumors. For example, it has long been recognized that solid tumors frequently contain hypoxic regions (65). Lack of oxygen leads to inhibition of hypoxia-inducible factor (HIF) prolylhydroxylase, a Fe(II) and 2OG-dependent dioxygenase (66). Hypoxic solid tumors also accumulate fumarate and/or succinate, which act as 2-oxoglutarate analogs and inhibit HIF prolylhydroxylase (67, 68). In such tumors, alkylation-specific Fe(II)/2OG-dependent demethylases may also be inhibited just like HIF prolylhydroxylase, and such tumors may actually be dependent on alkylation-specific DNA glycosylases for damage removal and BER for single strand break repair. Our genetic analysis indicates that, when only the TLS polymerase Polζ was present, it failed to substitute for the role of both the oxidative demethylase Tpa1 and the alkyl base glycosylase Mag1 in *S. cerevisiae*. We speculate that, in such situations, alkylation by MMS would cause multiple fork-blocking lesions on DNA during S phase, giving alkylating drugs a much greater impact. In checkpoint-deficient tumor cells and checkpoint-mutant yeast strains (69, 70), such fork stalling would be irreversible, and the stretches of DNA between collapsed forks would remain unreplicated at the end of S phase. When such cells complete mitosis, it would result in catastrophic chromosome breakage and rearrangement. In this regard, future work will include the study of repair pathways in clinically relevant chemotherapeutic drugs, including alkylating agents.

Acknowledgments—We thank Dr. Hans Krokan (Norwegian University of Science and Technology) for E. coli HK82 (*alkB*) cells.

REFERENCES

1. Rajski, S. R., and Williams, R. M. (1998) DNA cross-linking agents as antitumor drugs. *Chem. Rev.* **98,** 2723–2796
2. Beranek, D. T. (1990) Distribution of methyl and ethyl adducts following alkylation with monofunctional alkylating agents. *Mutat. Res.* **231,** 11–30
3. Singer, B., and Grunberger, D. (1983) molecular biology of mutagens and carcinogens, Plenum Publishing Corp., New York
4. Sedgwick, B. (2004) Repairing DNA-methylation damage. *Nat. Rev. Mol. Cell Biol.* **5,** 148–157
5. Johnson, R. E., Yu, S. L., Prakash, S., and Prakash, L. (2007) A role for yeast and human translesion synthesis DNA polymerases in promoting replication through 3-methyl adenine. *Mol. Cell Biol.* **27,** 7198–7205
6. Kunz, B. A., Straffon, A. F., and Vonarx, E. J. (2000) DNA damage-induced mutation: tolerance via translesion synthesis. *Mutat. Res.* **451,** 169–185
7. Washington, M. T., Johnson, R. E., Prakash, S., and Prakash, L. (2000) Accuracy of thymine-thymine dimer bypass by *Saccharomyces cerevisiae* DNA polymerase η. *Proc. Natl. Acad. Sci. U.S.A.* **97,** 3094–3099
8. Acharya, N., Johnson, R. E., Prakash, S., and Prakash, L. (2006) Complex formation with Rev1 enhances the proficiency of *Saccharomyces cerevisiae* DNA polymerase ζ for mismatch extension and for extension opposite from DNA lesions. *Mol. Cell Biol.* **26,** 9555–9563
9. Falnes, P. Ø., Bjørås, M., Aas, P. A., Sundheim, O., and Seeberg, E. (2004) Substrate specificities of bacterial and human AlkB proteins. *Nucleic Acids Res.* **32,** 3456–3461
10. Falnes, P. Ø. (2004) Repair of 3-methylthymine and 1-methylguanine lesions by bacterial and human AlkB proteins. *Nucleic Acids Res.* **32,** 6260–6267
11. Delaney, J. C., and Essigmann, J. M. (2004) Mutagenesis, genotoxicity, and repair of 1-methyladenine, 3-alkylcytosines, 1-methylguanine, and 3-methylthymine in alkB *Escherichia coli*. *Proc. Natl. Acad. Sci. U.S.A.* **101,** 14051–14056
12. Falnes, P. Ø., Klungland, A., and Alseth, I. (2007) Repair of methyl lesions in DNA and RNA by oxidative demethylation. *Neuroscience* **145,** 1222–1232
13. Trewick, S. C., Henshaw, T. F., Hausinger, R. P., Lindahl, T., and Sedgwick, B. (2002) Oxidative demethylation by *Escherichia coli* AlkB directly reverts DNA base damage. *Nature* **419,** 174–178
14. Aas, P. A., Otterlei, M., Falnes, P. O., Vågbø, C. B., Skorpen, F., Akbari, M.,

Sundheim, O., Bjørås, M., Slupphaug, G., Seeberg, E., and Krokan, H. E. (2003) Human and bacterial oxidative demethylases repair alkylation damage in both RNA and DNA. *Nature* **421,** 859–863
15. Ougland, R., Zhang, C. M., Liiv, A., Johansen, R. F., Seeberg, E., Hou, Y. M., Remme, J., and Falnes, P. Ø. (2004) AlkB restores the biological function of mRNA and tRNA inactivated by chemical methylation. *Mol. Cell* **16,** 107–116
16. Kurowski, M. A., Bhagwat, A. S., Papaj, G., and Bujnicki, J. M. (2003) Phylogenomic identification of five new human homologs of the DNA repair enzyme AlkB. *BMC Genomics* **4,** 48
17. Gerken, T., Girard, C. A., Tung, Y. C., Webby, C. J., Saudek, V., Hewitson, K. S., Yeo, G. S., McDonough, M. A., Cunliffe, S., McNeill, L. A., Galvanovskis, J., Rorsman, P., Robins, P., Prieur, X., Coll, A. P., Ma, M., Jovanovic, Z., Farooqi, I. S., Sedgwick, B., Barroso, I., Lindahl, T., Ponting, C. P., Ashcroft, F. M., O'Rahilly, S., and Schofield, C. J. (2007) The obesity-associated FTO gene encodes a 2-oxoglutarate-dependent nucleic acid demethylase. *Science* **318,** 1469–1472
18. Sedgwick, B., Bates, P. A., Paik, J., Jacobs, S. C., and Lindahl, T. (2007) Repair of alkylated DNA: recent advances. *DNA Repair* **6,** 429–442
19. Wei, Y. F., Chen, B. J., and Samson, L. (1995) Suppression of *Escherichia coli* alkB mutants by *Saccharomyces cerevisiae* genes. *J. Bacteriol.* **177,** 5009–5015
20. Choudhary, V., and Schneiter, R. (2012) Pathogen-related yeast (PRY) proteins and members of the CAP superfamily are secreted sterol-binding proteins. *Proc. Natl. Acad. Sci. U.S.A.* **109,** 16882–16887
21. Verna, J., Lodder, A., Lee, K., Vagts, A., and Ballester, R. (1997) A family of genes required for maintenance of cell wall integrity and for the stress response in *Saccharomyces cerevisiae*. *Proc. Natl. Acad. Sci. U.S.A.* **94,** 13804–13809
22. Aravind, L., and Koonin, E. V (2001) The DNA-repair protein AlkB, EGL-9, and leprecan define new families of 2-oxoglutarate- and iron-dependent dioxygenases. *Genome Biol.* **2,** RESEARCH0007
23. Keeling, K. M., Salas-Marco, J., Osherovich, L. Z., and Bedwell, D. M. (2006) Tpa1p is part of an mRNP complex that influences translation termination, mRNA deadenylation, and mRNA turnover in *Saccharomyces cerevisiae*. *Mol. Cell Biol.* **26,** 5237–5248
24. Henri, J., Rispal, D., Bayart, E., van Tilbeurgh, H., Séraphin, B., and Graille, M. (2010) Structural and functional insights into *Saccharomyces cerevisiae* Tpa1, a putative prolylhydroxylase influencing translation termination and transcription. *J. Biol. Chem.* **285,** 30767–30778
25. Kim, H. S., Kim, H. L., Kim, K. H., Kim do, J., Lee, S. J., Yoon, J. Y., Yoon, H. J., Lee, H. Y., Park, S. B., Kim, S. J., Lee, J. Y., and Suh, S. W. (2010) Crystal structure of Tpa1 from *Saccharomyces cerevisiae*, a component of the messenger ribonucleoprotein complex. *Nucleic Acids Res.* **38,** 2099–2110
26. Loenarz, C., Sekirnik, R., Thalhammer, A., Ge, W., Spivakovsky, E., Mackeen, M. M., McDonough, M. A., Cockman, M. E., Kessler, B. M., Ratcliffe, P. J., Wolf, A., and Schofield, C. J. (2014) Hydroxylation of the eukaryotic ribosomal decoding center affects translational accuracy. *Proc. Natl. Acad. Sci. U.S.A.* **111,** 4019–4024
27. Hanway, D., Chin, J. K., Xia, G., Oshiro, G., Winzeler, E. A., and Romesberg, F. E. (2002) Previously uncharacterized genes in the UV- and MMS-induced DNA damage response in yeast. *Proc. Natl. Acad. Sci. U.S.A.* **99,** 10605–10610
28. Choi, Y., Sims, G. E., Murphy, S., Miller, J. R., and Chan, A. P. (2012) Predicting the functional effect of amino acid substitutions and indels. *PLoS ONE* **7,** e46688
29. Schymkowitz, J., Borg, J., Stricher, F., Nys, R., Rousseau, F., and Serrano, L. (2005) The FoldX web server: an online force field. *Nucleic Acids Res.* **33,** W382–8
30. Westbye, M. P., Feyzi, E., Aas, P. A., Vågbø, C. B., Talstad, V. A., Kavli, B., Hagen, L., Sundheim, O., Akbari, M., Liabakk, N. B., Slupphaug, G., Otterlei, M., and Krokan, H. E. (2008) Human AlkB homolog 1 is a mitochondrial protein that demethylates 3-methylcytosine in DNA and RNA. *J. Biol. Chem.* **283,** 25046–25056
31. Korvald, H., Falnes, P. Ø., Laerdahl, J. K., Bjørås, M., and Alseth, I. (2012) The *Schizosaccharomyces pombe* AlkB homolog Abh1 exhibits AP lyase activity but no demethylase activity. *DNA Repair* **11,** 453–462
32. Anindya, R., Mari, P. O., Kristensen, U., Kool, H., Giglia-Mari, G., Mullenders, L. H., Fousteri, M., Vermeulen, W., Egly, J. M., and Svejstrup, J. Q. (2010) A ubiquitin-binding domain in Cockayne syndrome B required for transcription-coupled nucleotide excision repair. *Mol. Cell* **38,** 637–648
33. Henshaw, T. F., Feig, M., and Hausinger, R. P. (2004) Aberrant activity of the DNA repair enzyme AlkB. *J. Inorg. Biochem.* **98,** 856–861
34. Anindya, R., Aygün, O., and Svejstrup, J. Q. (2007) Damage-induced ubiquitylation of human RNA polymerase II by the ubiquitin ligase Nedd4, but not Cockayne syndrome proteins or BRCA1. *Mol. Cell* **28,** 386–397
35. Shivange, G., Kodipelli, N., and Anindya, R. (2014) A nonradioactive restriction enzyme-mediated assay to detect DNA repair by Fe(II)/2-oxoglutarate-dependent dioxygenase. *Anal. Biochem.* **465C,** 35–37
36. Li, Q., Sritharathikhun, P., and Motomizu, S. (2007) Development of novel reagent for Hantzsch reaction for the determination of formaldehyde by spectrophotometry and fluorometry. *Anal. Sci.* **23,** 413–417
37. Thomas, B. J., and Rothstein, R. (1989) Elevated recombination rates in transcriptionally active DNA. *Cell* **56,** 619–630
38. Taschner, M., Harreman, M., Teng, Y., Gill, H., Anindya, R., Maslen, S. L., Skehel, J. M., Waters, R., and Svejstrup, J. Q. (2010) A role for checkpoint kinase-dependent Rad26 phosphorylation in transcription-coupled DNA repair in Saccharomyces cerevisiae. *Mol. Cell Biol.* **30,** 436–446
39. Sikorski, R. S., and Hieter, P. (1989) A system of shuttle vectors and yeast host strains designed for efficient manipulation of DNA in *Saccharomyces cerevisiae*. *Genetics* **122,** 19–27
40. Petrov, A. N., Meskauskas, A., Roshwalb, S. C., and Dinman, J. D. (2008) Yeast ribosomal protein L10 helps coordinate tRNA movement through the large subunit. *Nucleic Acids Res.* **36,** 6187–6198
41. Kataoka, H., Yamamoto, Y., and Sekiguchi, M. (1983) A new gene (alkB) of *Escherichia coli* that controls sensitivity to methyl methane sulfonate. *J. Bacteriol.* **153,** 1301–1307
42. Dinglay, S., Trewick, S. C., Lindahl, T., and Sedgwick, B. (2000) Defective processing of methylated single-stranded DNA by *E. coli* AlkB mutants. *Genes Dev.* **14,** 2097–2105
43. Spence, E. L., Kawamukai, M., Sanvoisin, J., Braven, H., and Bugg, T. D. (1996) Catechol dioxygenases from *Escherichia coli* (MhpB) and *Alcaligenes eutrophus* (MpcI): sequence analysis and biochemical properties of a third family of extradiol dioxygenases. *J. Bacteriol.* **178,** 5249–5256
44. Eichhorn, E., van der Ploeg, J. R., Kertesz, M. A., and Leisinger, T. (1997) Characterization of α-ketoglutarate-dependent taurine dioxygenase from *Escherichia coli*. *J. Biol. Chem.* **272,** 23031–23036
45. Simmons, J. M., Koslowsky, D. J., and Hausinger, R. P. (2012) Characterization of a *Trypanosoma brucei* Alkb homolog capable of repairing alkylated DNA. *Exp. Parasitol.* **131,** 92–100
46. Bjørnstad, L. G., Zoppellaro, G., Tomter, A. B., Falnes, P. Ø., and Andersson, K. K. (2011) Spectroscopic and magnetic studies of wild-type and mutant forms of the Fe(II)- and 2-oxoglutarate-dependent decarboxylase ALKBH4. *Biochem. J.* **434,** 391–398
47. Falnes, P. Ø., Johansen, R. F., and Seeberg, E. (2002) AlkB-mediated oxidative demethylation reverses DNA damage in *Escherichia coli*. *Nature* **419,** 178–182
48. Chen, H., and Costa, M. (2009) Iron- and 2-oxoglutarate-dependent dioxygenases: an emerging group of molecular targets for nickel toxicity and carcinogenicity. *Biometals* **22,** 191–196
49. Xiao, M., Yang, H., Xu, W., Ma, S., Lin, H., Zhu, H., Liu, L., Liu, Y., Yang, C., Xu, Y., Zhao, S., Ye, D., Xiong, Y., and Guan, K. L. (2012) Inhibition of α-KG-dependent histone and DNA demethylases by fumarate and succinate that are accumulated in mutations of FH and SDH tumor suppressors. *Genes Dev.* **26,** 1326–1338
50. Couture, J. F., Collazo, E., Ortiz-Tello, P. A., Brunzelle, J. S., and Trievel, R. C. (2007) Specificity and mechanism of JMJD2A, a trimethyllysine-specific histone demethylase. *Nat. Struct. Mol. Biol.* **14,** 689–695
51. Ma, W., Resnick, M. A., and Gordenin, D. A. (2008) Apn1 and Apn2 endonucleases prevent accumulation of repair-associated DNA breaks in budding yeast as revealed by direct chromosomal analysis. *Nucleic Acids Res.* **36,** 1836–1846
52. Svilar, D., Dyavaiah, M., Brown, A. R., Tang, J. B., Li, J., McDonald, P. R., Shun, T. Y., Braganza, A., Wang, X. H., Maniar, S., St Croix, C. M., Lazo, J. S., Pollack, I. F., Begley, T. J., and Sobol, R. W. (2012) Alkylation sensi-

tivity screens reveal a conserved cross-species functionome. *Mol. Cancer Res.* **10,** 1580–1596
53. Moazed, D., and Noller, H. F. (1987) Interaction of antibiotics with functional sites in 16 S ribosomal RNA. *Nature* **327,** 389–394
54. Röther, S., and Strässer, K. (2007) The RNA polymerase II CTD kinase Ctk1 functions in translation elongation. *Genes Dev.* **21,** 1409–1421
55. Duncan, T., Trewick, S. C., Koivisto, P., Bates, P. A., Lindahl, T., and Sedgwick, B. (2002) Reversal of DNA alkylation damage by two human dioxygenases. *Proc. Natl. Acad. Sci. U.S.A.* **99,** 16660–16665
56. Lee, D. H., Jin, S. G., Cai, S., Chen, Y., Pfeifer, G. P., and O'Connor, T. R. (2005) Repair of methylation damage in DNA and RNA by mammalian AlkB homologues. *J. Biol. Chem.* **280,** 39448–39459
57. John, S., Howe, L., Tafrov, S. T., Grant, P. A., Sternglanz, R., and Workman, J. L. (2000) The something about silencing protein, Sas3, is the catalytic subunit of NuA3, a yTAF(II)30-containing HAT complex that interacts with the Spt16 subunit of the yeast CP (Cdc68/Pob3)-FACT complex. *Genes Dev.* **14,** 1196–1208
58. Rout, M. P., and Aitchison, J. D. (2001) The nuclear pore complex as a transport machine. *J. Biol. Chem.* **276,** 16593–16596
59. Volkert, M. R., and Hajec, L. I. (1991) Molecular analysis of the aidD6::Mu d1 (bla lac) fusion mutation of *Escherichia coli* K12. *Mol. Gen. Genet.* **229,** 319–323
60. Xiao, W., Chow, B. L., and Rathgeber, L. (1996) The repair of DNA methylation damage in *Saccharomyces cerevisiae*. *Curr. Genet.* **30,** 461–468
61. Hendricks, C. A., Razlog, M., Matsuguchi, T., Goyal, A., Brock, A. L., and Engelward, B. P. (2002) The *S. cerevisiae* Mag1 3-methyladenine DNA glycosylase modulates susceptibility to homologous recombination. *DNA Repair* **1,** 645–659
62. Chang, M., Bellaoui, M., Boone, C., and Brown, G. W. (2002) A genome-wide screen for methyl methanesulfonate-sensitive mutants reveals genes required for S phase progression in the presence of DNA damage. *Proc. Natl. Acad. Sci. U.S.A.* **99,** 16934–16939
63. Calvo, J. A., Meira, L. B., Lee, C. Y., Moroski-Erkul, C. A., Abolhassani, N., Taghizadeh, K., Eichinger, L. W., Muthupalani, S., Nordstrand, L. M., Klungland, A., and Samson, L. D. (2012) DNA repair is indispensable for survival after acute inflammation. *J. Clin. Invest.* **122,** 2680–2689
64. Van Sloun, P. P., Varlet, I., Sonneveld, E., Boei, J. J., Romeijn, R. J., Eeken, J. C., and De Wind, N. (2002) Involvement of mouse Rev3 in tolerance of endogenous and exogenous DNA damage. *Mol. Cell Biol.* **22,** 2159–2169
65. Maxwell, P. H., Wiesener, M. S., Chang, G. W., Clifford, S. C., Vaux, E. C., Cockman, M. E., Wykoff, C. C., Pugh, C. W., Maher, E. R., and Ratcliffe, P. J. (1999) The tumour suppressor protein VHL targets hypoxia-inducible factors for oxygen-dependent proteolysis. *Nature* **399,** 271–275
66. Ivan, M., Kondo, K., Yang, H., Kim, W., Valiando, J., Ohh, M., Salic, A., Asara, J. M., Lane, W. S., and Kaelin, W. G., Jr. (2001) HIFα targeted for VHL-mediated destruction by proline hydroxylation: implications for O_2 sensing. *Science* **292,** 464–468
67. Isaacs, J. S., Jung, Y. J., Mole, D. R., Lee, S., Torres-Cabala, C., Chung, Y. L., Merino, M., Trepel, J., Zbar, B., Toro, J., Ratcliffe, P. J., Linehan, W. M., and Neckers, L. (2005) HIF overexpression correlates with biallelic loss of fumarate hydratase in renal cancer: novel role of fumarate in regulation of HIF stability. *Cancer Cell* **8,** 143–153
68. Selak, M. A., Armour, S. M., MacKenzie, E. D., Boulahbel, H., Watson, D. G., Mansfield, K. D., Pan, Y., Simon, M. C., Thompson, C. B., and Gottlieb, E. (2005) Succinate links TCA cycle dysfunction to oncogenesis by inhibiting HIF-α prolyl hydroxylase. *Cancer Cell* **7,** 77–85
69. Lopes, M., Cotta-Ramusino, C., Pellicioli, A., Liberi, G., Plevani, P., Muzi-Falconi, M., Newlon, C. S., and Foiani, M. (2001) The DNA replication checkpoint response stabilizes stalled replication forks. *Nature* **412,** 557–561
70. Tercero, J. A., and Diffley, J. F. (2001) Regulation of DNA replication fork progression through damaged DNA by the Mec1/Rad53 checkpoint. *Nature* **412,** 553–557